Proceedings of the 21st ICSMGE, Vienna, Austria, 14 – 19 June 2026. Pistrol, Adam & Schweiger (eds.)
Published by: ÖGG, Austrian Society for Geomechanics, Salzburg, Austria, ISBN 978-3-9503898-4-5
https://doi.org/10.53243/ICSMGE2026-2257

Seismic Vulnerability Analysis of a CFRD Dam

Camilo Marulanda, William Ruíz
INGETEC, Bogotá, Colombia, marulanda@ingetec.com.co; wruiz@ingetec.com.co

ABSTRACT: This paper presents a comprehensive seismic vulnerability assessment of the Porce III Dam, a 151-meter-high Concrete-Faced Rockfill Dam (CFRD) with a volume of 4.2 million m³ located in northwestern Colombia. The primary objective was to rigorously evaluate the dam's dynamic response and global stability under extreme seismic events. The assessment commenced with a two-dimensional limit equilibrium model for initial safety factor estimation. Subsequently, a robust three-dimensional hybrid numerical model was developed, integrating Finite Difference (FLAC3D) and Finite Element (ABAQUS) methods. FLAC3D simulated the rockfill's nonlinear behavior and wave propagation, while ABAQUS utilized these inputs to analyze specific stresses within the concrete face and plinth interfaces. This hybrid approach was crucial for accurately modeling complex interactions while ensuring realistic material representations. Complemented by instrumentation data, the results demonstrate that the Porce III Dam possesses adequate safety margins. The results show that the Porce III dam has adequate safety margins against significant seismic demands, maintaining moderate displacements at the crest and avoiding critical cracking in the concrete face.

KEYWORDS: Concrete-Faced Rockfill Dam (CFRD), Numerical Modeling, Finite Element Models, Seismic Stability, Geotechnical Instrumentation, dynamic response.

1 INTRODUCTION

Concrete-Faced Rockfill Dams (CFRDs) typically exhibit favorable performance under seismic excitation because the dam body remains dry, preventing the generation of excess pore water pressures that could lead to strength degradation in the rockfill. Additionally, the reservoir exerts hydrostatic pressure across the entire surface of the concrete face, further stabilizing the dam body by increasing its confinement.

However, the seismic response of CFRDs remains an active area of research in engineering, as only a few of these dams have been subjected to design-level seismic loads. Consequently, only a limited number of cases provide reliable acceleration records and geotechnical instrumentation data necessary for detailed dynamic analysis and validation.

A notable exception is the Zipingpu Dam, located in the Sichuan region of China, which stands 156 meters high with a crest length of 663.8 meters. On May 12, 2008, the Wenchuan Earthquake occurred with an epicenter just 17 km from the dam, generating ground accelerations of up to 0.5g—significantly exceeding the design-level rock acceleration of 0.26g (Degao Zou, 2013). This event provided a unique opportunity to evaluate the seismic performance of CFRDs under such extreme acceleration levels. As a result, the dam crest experienced settlements of up to 1 meter, causing damage to the parapet wall and localized cracking in the concrete face. However, the overall stability of the dam was never compromised.

Additionally, during the February 6, 2023, earthquake and its aftershocks in Turkey, several CFRDs near the East Anatolian Fault experienced very high rock accelerations. Despite these extreme loading conditions, their performance was satisfactory, with no detectable structural damage observed in the dams or their concrete face elements.

These cases support the conclusion that properly designed and constructed CFRDs exhibit remarkable resilience to seismic loading. Furthermore, with modern computational capabilities, advanced numerical analyses can now be performed to better understand and evaluate the overall behavior of these structures under seismic conditions.

The dynamic response of CFRDs is influenced by multiple factors, including:

- Density and quality of the rockfill.
- Dam geometry.
- Canyon shape.
- Characteristics of joints between the slabs and plinth.
- Concrete reinforcement.
- Seismic parameters, such as duration, frequency content, and amplitude of ground motion.

2 SEISMIC HAZARD ASSESSMENT FOR THE PORCE III DAM

An updated seismic hazard analysis was performed for the Porce III dam to assess local fault activity and improve seismic response assessment. The study involved two main phases: (1) neotectonic studies to characterize local faults through geological surveys, review of existing data, and field investigations to identify recent fault activity in Quaternary deposits; and (2) probabilistic and deterministic seismic hazard analyses (PSHA and DSHA) to estimate peak ground and spectral acceleration values.

The seismic hazard analyses incorporated a seismic catalog from 1993 to 2020 and evaluated two scenarios using different Ground Motion Prediction Equations (GMPEs), including updated models developed after 2006.

As a sensitivity analysis, two seismic hazard scenarios were evaluated using different Ground Motion Prediction Equations (GMPEs) to assess the impact of varying attenuation laws. Scenario 1 applied a set of widely used GMPEs for crustal sources (Abrahamson, Silva & Kamai, 2014; Campbell & Bozorgnia, 2014; Chiou & Youngs, 2014) and for subduction and Benioff sources (Atkinson & Boore, 2003; Young et al., 1997; Zhao et al., 2006). Scenario 2 used GMPEs from the US2014 National Seismic Hazard Maps, which yielded higher and more critical spectral values. Figure 1 shows the SEE verification spectra for both scenarios, validating the representativeness of these signals and confirming their applicability in numerical modelling.

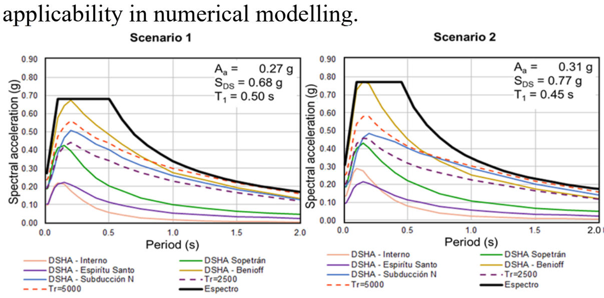

Figure 1. Seismic verification spectrum for the Safety Evaluation Earthquake (SEE) of Porce III dam.

3 DAM ZONING AND FOUNDATION CHARACTERISTICS

The Porce III Dam is a zoned rockfill structure composed of three main rockfill zones, each designed with specific material properties and placement techniques (See Figure 2).

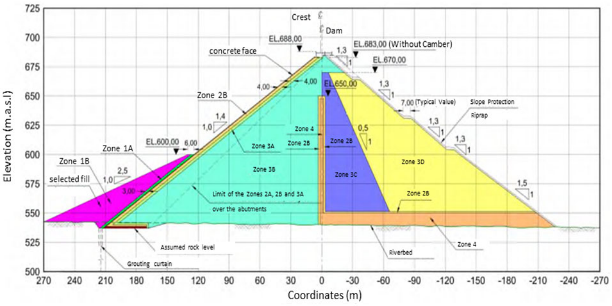

Figure 2. Cross section and dam zoning of Porce III Dam

Zone 3B, which forms the upstream shoulder and upper section of the dam, was constructed in 600 mm-thick layers using excavation spoil from underground works in the lower section, fresh schist (weathering grade III, from Deere and Patton (1969) from underground and spillway excavations in the middle section, and materials from spillway excavations in the upper portion. Zone 3C, the central core, consists of moderately to highly weathered schists compacted in 600 mm-thick layers, ensuring a dense and stable core. The downstream shoulder, Zone 3D, was built using the same materials as Zone 3C but with a thicker compaction layer of 900 mm, enhancing stability and structural integrity.

To control seepage, the dam incorporates a 3.0 m-wide chimney drain and a drainage blanket, designed to prevent water infiltration through the concrete face and keep the rockfill dry. These drainage structures were built using processed materials sourced from underground excavations and alluvial deposits (Zone 4). Additionally, filter and transition zones (2A, 2B, and 3A) were placed between the main rockfill zones and the fine-grained Zones 1A and 1B, which act as a sealing barrier against potential cracking in the concrete face under high hydrostatic pressures.

The foundation of the dam was constructed on quartz-graphitic schists (Pesgr), which exhibit varying degrees of weathering depending on the location. On the left abutment, the upper section consists of moderately weathered (IIB) quartz-graphitic schists, while the middle and lower sections rest on highly weathered (IIA) quartz schists. The right abutment (central area) is primarily founded on highly weathered (IIA) quartz schists, whereas the riverbed foundation transitions from moderately weathered (IIB) to fresh (III) quartz schists (Pesqz), ensuring a stable base for the dam structure.

Furthermore, the concrete face and plinth were extensively characterized using as-built drawings and quality control records. This detailed material assessment was crucial for incorporating realistic material properties into the numerical models, ensuring that the simulations accurately represent the dam's behavior under seismic loading.

4 BEHAVIOR AND NUMERICAL MODELLING OF THE CONCRETE FACE IN A CFRD

Due to its high slenderness, the concrete face slabs of a rockfill dam behave essentially as membranes under hydrostatic loading. This does not mean they are free of internal shear forces but rather that their out-of-plane deformation is controlled primarily by the deformation of the rockfill rather than by their own stiffness. In other words, their structural response is deformation-controlled rather than load-controlled. Consequently, the deformation of the slab is largely independent of the concrete material properties and reinforcement details, being instead strongly influenced by the stiffness of the rockfill and geometric factors.

A numerical model of the concrete face must incorporate all relevant mechanisms affecting its behavior, including:

- Friction and separation between the plinth and the slabs.
- Three-dimensional deformations experienced by the concrete face during construction and reservoir filling.

Due to the lack of analytical solutions that account for all these mechanisms and until recently, the absence of computational tools capable of fully capturing these effects the design of CFRD concrete faces has traditionally relied on empirical methods and general design rules. A reflection of this approach is the determination of concrete slab thickness, which has been historically based on precedents rather than first-principles analysis.

The slab thickness has typically been determined as a function of reservoir pressure, initially following the empirical formula: $e = 0.30 + 0.003\, H$ where "e" is the slab thickness (m) and "H" is the reservoir height (m). In some cases, alternative formulas such as $e=0.30+0.002H$ have been used, and for dams under 120 m in height, even $e=0.30+0.001H$ has been applied. Additionally, in CFRD designs, reinforcement ratios have traditionally been around 0.5%, though this has gradually decreased to 0.4% and even 0.3% over time.

The recent trend of cost reduction in high CFRDs (>150 m) has led to elimination of anti-spalling reinforcement at compression joints, further reductions in slab thickness, and, in low-seismicity regions, increased upstream slope inclinations to 1.30H:1.0V and even 1.35H:1.0V, even for very tall dams. Over the past decades, there has been a significant increase in CFRD heights, largely driven by the assumption that, after the construction of Aguamilpa Dam (187 m high), increasing rockfill dam height would not pose major issues. However, it is important to emphasize that Aguamilpa is a gravel dam, which experiences significantly lower deformations than expected in a rockfill dam. As a result, simply extrapolating existing precedents has, in some cases, proven inadequate.

Thus, it is critical that CFRD designs, especially those involving height extrapolations based on precedents, be complemented by numerical tools that can accurately predict the behavior of individual components, particularly in terms of slab deformations, stresses, and crack development.

5 LOAD TRANSFER AND STRESS DEVELOPMENT IN THE CONCRETE FACE

While the deformation of the concrete face is primarily controlled by the rockfill, this is only true in the direction perpendicular to the face. It is important to also consider sliding at the interface between the rockfill and the concrete slab.

The mechanism for transferring loads from the rockfill to the concrete face is friction at the interface, which depends on the contact conditions. The maximum shear stress that can be transferred by friction is governed by:

- The normal pressure acting on the contact surface.
- The friction coefficient, which is influenced by contact roughness and material properties.

When the maximum shear strength is exceeded, sliding occurs, preventing further load transfer beyond this threshold.

In addition to interface frictional stresses, bending stresses develop in the concrete slabs, primarily due to the irregular foundation profile behind the face. The geometric configuration of the slab, which is supported on an inclined slope and, in some cases, within narrow canyons, also generates compressive forces due to self-weight load transfer.

Under hydrostatic loading, the concrete face undergoes deformation characterized by compression in the central region and tension toward its perimeter, the latter being reflected in the opening of perimeter joints.

6 NUMERICAL MODELLING FOR STRESS ANALYSIS IN THE CONCRETE FACE

To accurately evaluate the stresses developed in the concrete face, a detailed numerical model was developed, incorporating the various mechanisms that induce stress due to face movements in response to rockfill settlements from self-weight loading, deformations caused by reservoir load, and seismic loading effects.

Numerical analysis of a Concrete-Faced Rockfill Dam (CFRD) provides valuable insights into its overall behavior and key performance aspects, offering approximate values for critical variables such as stress distribution, deformations and strain patterns, and crack widths and potential seepage pathways. However, given the complexity of the system, it is unrealistic to expect numerical models to deliver exact and highly detailed results.

For the seismic vulnerability assessment of the Porce III Dam, nonlinear dynamic analyses were conducted using a three-dimensional finite difference model developed in FLAC3D, which accounted for the dam foundation, rockfill zones, and plinth. Additionally, a finite element sub model was developed in Abaqus CAE, specifically modeling the plinth, concrete face, and its interactions with the plinth and parapet wall to better capture local stress concentrations and deformation behaviors.

6.1 *Modelling Assumptions and Simplifications*

As with the limit equilibrium model, the zoning of the rockfill was simplified to include only the three main zones (3B, 3C, and 3D). This simplification was based on the understanding that these zones primarily govern the stress-strain behavior of the dam body, which is the focus of the analysis. Consequently, the filter and drainage layer (Zone 4) were not explicitly modeled.

As previously discussed, the dam foundation consists of quarzitic and quartz-graphitic schists, ranging from highly weathered to fresh conditions. These materials exhibit stiffness and strength values significantly higher than those of the rockfill, meaning their influence on the dynamic response of the dam is minimal. However, the foundation was still included in the model to ensure that boundary conditions were applied on smooth surfaces, allowing for the implementation of absorbing and free-field boundary conditions. For simplicity, the foundation was modeled as a single high-stiffness material.

Figure 3 illustrates the finite difference and finite element model assembly. Each concrete slab of the dam face was treated as an independent body, allowing for contact interactions between slabs and between the slab and the plinth. This setup enables sliding and separation at the interfaces, capturing the realistic interaction between the concrete face and rockfill.

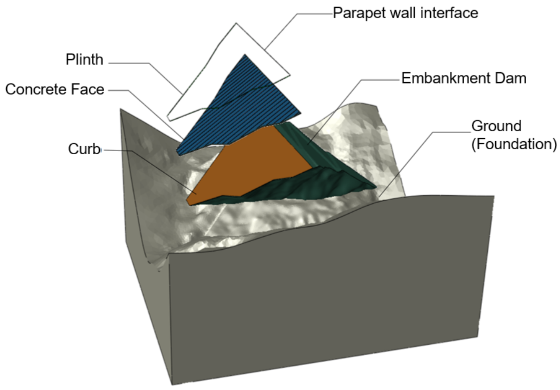

Figure 3. Assembly for the numerical models

The interaction between the rockfill model and the concrete face sub model was achieved by mapping deformations from the plinth (the common element) between the finite difference model and the finite element model using custom subroutines. The selection of these programs and workflow was because FLAC3D provides the appropriate constitutive models to accurately represent the dynamic behavior of rockfill materials, as well as absorbing and free-field boundary conditions, which enable a realistic simulation of seismic wave propagation.

On the other hand, Abaqus CAE allows for the modeling of frictional contacts between individual concrete slabs, as well as between the concrete face, plinth, and curb. Additionally, this multi-purpose finite element software enables the inclusion of reinforcement within the slabs through embedded reinforcement elements. Moreover, it features the Concrete Damage Plasticity (CDP) model, which allows for the consideration of nonlinear and cyclic behavior of concrete, including the estimation of tensile cracking in the slabs.

6.2 *Calibration of the Numerical Model*

To assess the current behavior of the CFRD Porce III dam using the three-dimensional numerical model, the model was calibrated by simulating the construction process with the staged construction sequence. Additionally, a force was applied to the upstream shoulder to simulate the overload of zones 1A and 1B, as well as the hydrostatic load from the reservoir filling up to EL. 667.0 masl, which corresponds to the reservoir level most frequently recorded during the project's operation.

The settlements recorded by the numerical model were compared with those measured by the dam's instrumentation. This comparison was conducted for settlement readings from the start of dam construction (2007) until February 2023 for the RMVs or until the last reading deemed reliable for the settlement cells.

The total maximum settlements, occurs in the downstream shoulder in Zone 3D, reaching 2.33 m at EL 620.0 masl, considering those that occurred during the construction of the dam, the overload of zones 1A and 1B on the upstream shoulder, and the first filling of the reservoir (See Figure 4). On the other hand, the settlements on the upstream shoulder face are below 1.0 m.

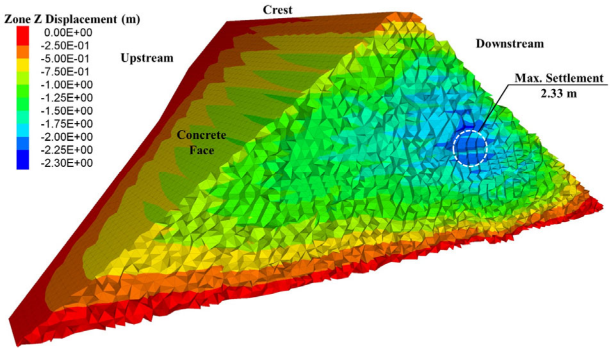

Figure 4. Settlement (m) at the end of reservoir filling - representative of the current deformation.

Comparisons of the settlements obtained in the numerical model through the simulation of the dam construction process and reservoir filling with the values recorded by the existing geotechnical instrumentation were performed with differences generally less than 0.1 m, a value considered acceptable since, due to the mesh size, the settlements cannot be compared at the exact location of each instrument. The good agreement in the settlements of the instruments located further upstream is highlighted, which are key to adequately representing the behavior of the concrete face.

Table 1 presents the adjusted parameters of the Plastic Hardening model for the three zones of the dam considered in the model, which provided the best fit to the previously presented settlement readings from the instrumentation. These calibrated parameters highlight a significant difference in both modulus and strength parameters between the upstream Zone 3B and Zone 3D. This difference is consistent with the more weathered schists used in the latter zone and the lower compaction requirements.

Table 1. Calibrated parameters of the Plastic Hardening Model

Parameter	Zone 3B	Zone 3C	Zone 3D
$E_{50}{}^{ref}$ (MPa)	28	23	17
$E_{eod}{}^{ref}$ (MPa)	17,3	12,1	7,6
$E_{ur}{}^{ref}$ (MPa)	113	92	67,3
R_f (--)	0,59	0,66	0,59
$p_p{}^{ref}$ (kPa)	100	100	100
m (--)	0,37	0,46	0,46
φ'_0 (°)	58,4	54,4	44,0
$\Delta\varphi'$ (°)	13,4	7,7	8,2

Since the numerical model was calibrated using settlement readings from the construction of the dam up to the last reliable reading from each instrument, it indirectly accounts for the settlements that occurred after the reservoir was filled. Therefore, it can be used to evaluate the current condition of the Porce III CFRD dam.

Figure 5 presents the major principal stress $\sigma 1$ (more compressive) and the minor principal stress $\sigma 3$ (less compressive) in the dam's maximum section, providing insight into the current stress levels within the dam body.

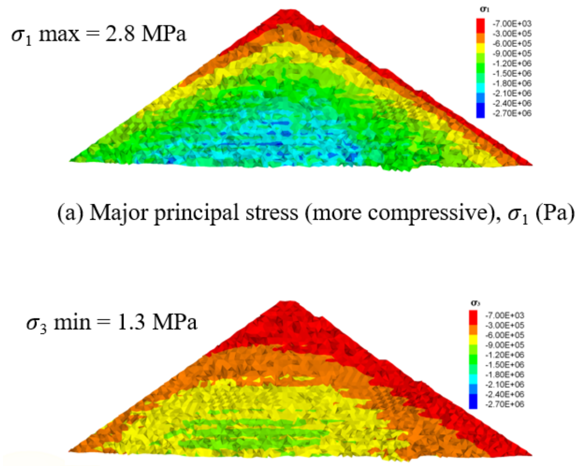

(a) Major principal stress (more compressive), σ_1 (Pa)

(b) Minor principal stress (less compressive), σ_3 (Pa)

Figure 5. Current principal stresses in the dam's maximum section

The highest stresses occur in the lower part of Zone 3B due to greater confinement from the weight of the fill materials and the reservoir load. In this area, the major principal stresses reach values of up to 2.8 MPa, while the minor principal stresses are below 1.3 MPa.

Regarding the concrete face of the dam, Figure 6 shows the deformation caused by the overload of zones 1A and 1B and the hydrostatic pressure from the reservoir. As observed in this figure and consistent with the expected behavior of concrete-faced dams, the greatest displacement occurs in the lower third, near elevation EL. 580.0 masl, and towards the center of the river canyon. This is where the fill height is greatest (and therefore has lower stiffness) compared to the abutments, which have greater stiffness due to the proximity of the foundation rock.

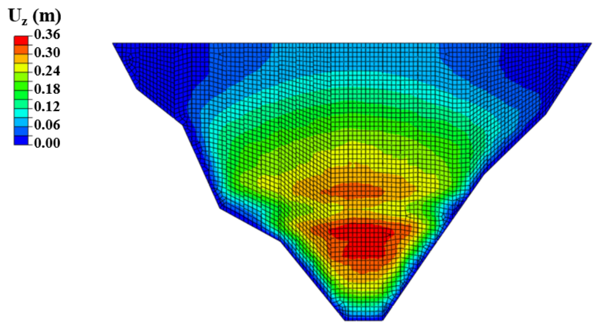

Figure 6. Displacement (m) of the concrete face under reservoir loads and zones 1A and 1B

6.3 *Seismic induced deformations*

The seismic performance of concrete-faced rockfill dams has historically been satisfactory. Even the Zipingpu Dam, which was subjected to rock accelerations up to twice the design PGA and experienced crest settlements of 1 meter as well as significant damage to the construction joint of the concrete face, performed adequately during and after the earthquake. More recently, during the February 6, 2023, earthquake in Turkey, several dams in the country were exposed to very high rock accelerations that induced high accelerations at the crest, yet they also performed well during and after the earthquake.

The historical performance of concrete-faced rockfill dams also allows for estimating the levels of amplification and crest settlement that can be expected given the occurrence of earthquakes of various magnitudes and peak ground accelerations (PGA). ICOLD Bulletin 141 (ICOLD, 2012) presents historical data on the behavior of several CFRD dams during earthquakes of varying intensities, defining intensity as:

$$ESI = PGA\,(M - 4.5)^3 \quad (1)$$

For the Porce III dam, this corresponds to an ESI value of 9.34 and crest settlements ranging between 0.15%H and 0.45%H, or approximately 21 cm to 63 cm. Additionally, seismic records collected from embankment dams (rockfill and earthfill) that have been subjected to significant-magnitude earthquakes allow for establishing a relationship between peak ground acceleration (PGA) on rock and the maximum amplification expected in this type of dam.

The data indicates that for an earthquake with a PGA of 0.26g, an amplification factor of approximately 2.2 can be expected. These values are useful and serve as an initial reference for interpreting the results of the numerical analyses presented in the following section.

6.4 *Numerical analysis results*

The three-dimensional numerical model for nonlinear dynamic analyses starts from a stress state that approximates the current condition of the dam, with the reservoir level at EL. 667.0 masl. This stress state was achieved by simulating the construction process in a simplified manner and applying the hydrostatic load generated by the reservoir filling as described previously. The simulation of the construction stages and reservoir filling was carried out using the Plastic Hardening model, with calibrated parameters for each zone based on settlement readings recorded by the instrumentation. This procedure was described in the previous section.

The nonlinear dynamic analyses were performed using the ground motion that produces the highest settlements according to the Simplified deformation analysis methodology (Makdisi & Seed, 1978; Bray & Travasarou, 2011). The constitutive model was used with hysteretic damping, calibrated to reproduce the degradation of the modulus and the representative damping for the dam material.

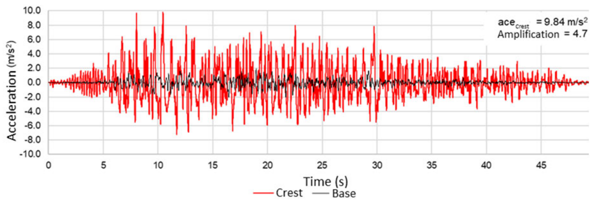

(a) Acceleration records over time at the foundation level (base) and at the dam crest.

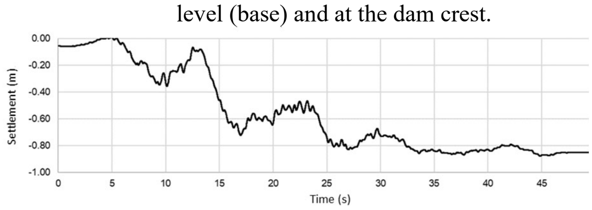

(b) Crest settlement over time

Figure 7. Horizontal acceleration (perpendicular to the dam axis) at the crest and base of the model, and settlement at the crest.

The results are presented in Figure 7. The maximum acceleration at the crest for this analysis condition is 9.84 m/s² (see Figure 7a), corresponding to an amplification factor of 4.7. The maximum expected deformation in this case is 0.85 m (see Figure 7b), while the shear strain is 3.3%, both occurring on the downstream shoulder towards the right abutment at the height of the first access ramp. The maximum settlement at the crest is 85 cm.

Previously an empirical estimate was presented based on historical data collected from concrete-faced dams subjected to significant-magnitude earthquakes, estimating a maximum crest deformation of 63 cm. Simplified analyses were conducted to estimate earthquake-induced deformations, where a maximum deformation of 15.3 cm was estimated on the downstream shoulder. In contrast, the finite difference analysis—based on a meticulous calibration process of modulus values and the dynamic characteristics of the materials in the Porce III dam, and utilizing state-of-the-practice numerical analysis methodologies estimated a maximum crest deformation of 85 cm.

The historical experience of concrete-faced rockfill dams allows for estimating the amplification of seismic waves as a function of the expected PGA on rock in a numerical analysis. Specifically, ICOLD Bulletin 141 presents a compilation of experiences indicating that for rock signals of 0.26g, an amplification of approximately 2.2 can be expected. However, the analyses show an amplification of 4.7, more than double the value reported in the literature.

To understand why the analysis may be generating excessive amplification, it is important to highlight that the amplification of a seismic signal between the base and the crest of the dam in the numerical model depends, among other factors, on the following variables:

- The damping sources in the model (Rayleigh and hysteretic damping).
- The mass and stiffness matrices of the dam (density and shear stiffness modules).
- The absorbing boundaries at the base of the model and the free-field boundaries at the lateral edges.
- The geometry of the model (e.g., canyon shape).

When a model exhibits high amplification, it is possible that it is underestimating damping. In this case, the damping configuration is considered within the range of values reported in the literature and based on the author's experience with the dam materials. There may be additional sources of damping, such as the effect of the reservoir, which could mitigate the amplification of seismic waves in the model. Clearly, the estimated amplification in the numerical model developed in this study is higher than what has been historically recorded; however, it remains on the conservative side, allowing for an assessment of the dam's vulnerability under these elevated values. Since the analysis concluded that the dam could withstand these loads, it was not deemed necessary to refine the damping sources to reduce the estimated amplification.

Additionally, the calibration of the shear stiffness modules was carried out using the best available data for the analyses. However, there is some uncertainty in the final calibration of the dynamic modules, as the fundamental frequency of the dam was taken as 2.2 Hz based on the information reported by the owner of the dam, but the original data was not available for review. It is also possible that some aspects of the numerical model configuration are inducing the high signal amplification observed in the results. Nevertheless, as previously mentioned, the results obtained are on the conservative side, ensuring a safety margin in the assessment of the dam's performance.

6.5 *Deformation and cracking in the concrete face*

The concrete face of the Porce III dam has been modeled using a sub model in Abaqus CAE, which is coupled to the deformation of the curb in the finite difference model developed in FLAC3D. This hybrid approach assumes that the deformations of the dam under reservoir and seismic loads are approximately independent of the detailed behavior of the concrete face, such as joint opening and closing. In other words, the coupling between the concrete face and the dam is one-way: the dam's deformations serve as a time-dependent boundary condition for the concrete face and are applied in the Abaqus.

This hybrid provides several advantages for numerical modeling, including reducing model size, computational resource demands, and simulation time. Additionally, it allows the time step of the concrete face model to be independent of the dam model. Due to the small size of certain elements in the concrete face (e.g., four elements through the slab thickness), incorporating these elements into the dam model would excessively restrict the time step in the dam simulation.

In this finite element model (Abaqus CAE), the plinth and parapet provide contact for the concrete face against a hard material (wood, with a modulus of approximately 10 GPa and a thickness of 3 cm). The displacements of these components are assumed to be equal to those of the nearest elements: the plinth is fixed to the rock, and the parapet is fixed to the crest.

The results for total displacements in the concrete face, joint opening and closing, and crack width estimation at the end of the earthquake, the maximum displacement reaches 1.44 m at the upper part of the concrete face axis, in contact with the parapet wall. This result is consistent with the crest settlements of approximately 0.85 m, corresponding to the vertical displacement component (see Figure 8).

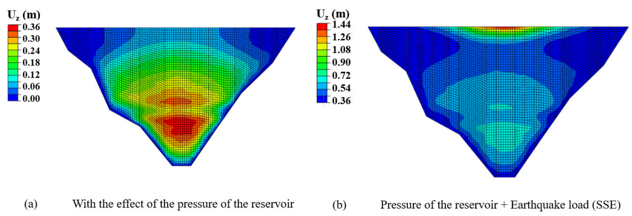

Figure 8. Total displacements in the concrete face, joint opening and closing, and crack width estimation at the end of the earthquake.

With the model, it was also possible to estimate the cracking zones in the concrete face and evaluate the behavior of the joints in terms of their opening and closing under seismic loading. By analyzing the stress distribution and deformation patterns, the model identified areas where tensile stresses exceeded the concrete's cracking threshold, providing insights into the potential locations and extent of cracking. Additionally, the simulation allowed for tracking the relative displacements of the joints, helping to determine whether they remained within acceptable movement ranges or if significant opening or closure occurred, which could affect the integrity of the concrete face.

These estimations are crucial for assessing the structural performance of the dam during an earthquake, as excessive joint movement or widespread cracking could compromise the watertightness and overall stability of the structure.

7 CONCLUSIONS

After calibrating the geotechnical properties of the materials that make up the fill body and concrete face of the Porce III dam, based on the behavior recorded by the instrumentation to date, and developing a hybrid numerical model that allowed for refining and obtaining a sufficiently detailed representation of the concrete face to evaluate its performance under stress demands and design conditions during the SEE earthquake, it is concluded that the dam behaves adequately, safely, and in compliance with the design criteria for which it was conceived, in accordance with the current state of engineering practice.

The amplification of seismic acceleration within the dam body is an uncertainty inherent to existing modeling methodologies. However, despite these limitations, the results obtained still represent a conservative scenario, as the calculated values are higher than those recorded in existing dams that have been subjected to high-intensity earthquakes. Even under these conditions, the Porce III dam is considered safe.

In conclusion, it is determined that the Porce III dam exhibits a stable seismic response within the design scenarios considered. The combination of numerical approaches and their validation with on-site instrumentation reaffirms the effectiveness of modeling methodologies for the safety evaluation of CFRD dams.

8 ACKNOWLEDGEMENTS

The authors express our gratefulness to EPM owner of Porce III Dam and all the staff from the Dam Safety unit for its support during this study and for granting permission to publish this article.

9 REFERENCES

Abrahamson, N., Silva, W., & Kamai, R. (2014). Summary of the ASK14 Ground Motion Relation for Active Crustal Regions. Earthquake Spectra, 30(3), 1025–1055.

Atkinson, G. M., & Boore, D. M. (2003). Empirical Ground Motion Relations for Subduction-Zone Earthquakes and Their Application to Cascadia and Other Regions. Bulletin of the Seismological Society of America, 93(4), 1703–1729.

Bray, J. D., & Travasarou, T. (2011). Pseudostatic Slope Stability Procedure for Earthquake-Induced Movements. Journal of Geotechnical and Geoenvironmental Engineering, 137(9), 957–971.

Campbell, K. W., & Bozorgnia, Y. (2014). NGA-West2 Campbell-Bozorgnia Ground Motion Model for the Average Horizontal Component of PGA, PGV, and 5%-Damped Linear Acceleration Response Spectra. Earthquake Spectra, 30(3), 1087–1115.

ICOLD (2012). Bulletin 141: Concrete Face Rockfill Dams – Concepts for Design and Construction. Paris, France, 2011, ISSN 0534-8293, E90·00, 401 pp.

Chiou, B. S. J., & Youngs, R. R. (2014). Update of the Chiou and Youngs NGA Model for the Average Horizontal Component of Peak Ground Motion and Response Spectra. Earthquake Spectra, 30(3), 1117–1153.

INGETEC (2021). Estudio de neotectónica y actualización de amenaza sísmica para las presas de los proyectos Porce II, Porce III, Playas, Río Grande I, Río Grande II y Santa Rita.

Makdisi, F. I., & Seed, H. B. (1978). Simplified Procedure for Estimating Dam and Embankment Earthquake-Induced Deformations. Journal of the Geotechnical Engineering Division, 104(GT7), 849–867.

Newmark, N. M. (1975). Effects of Earthquakes on Dams and Embankments. Géotechnique, 25(4), 139–159.

USGS (United States Geological Survey). (2014). National Seismic Hazard Maps - Data and Documentation. U.S. Department of the Interior, Washington, D.C.

Young, R. R., et al. (1997). Ground-Motion Parameters for Subduction Earthquakes in the Cascadia Region. Seismological Research Letters, 68(1), 58–73.

Zhao, J. X., et al. (2006). Attenuation Relations of Strong Ground Motion in Japan Using Site Classification Based on Predominant Period. Bulletin of the Seismological Society of America, 96(3), 898–913.

Zou, D., Xu, B., Kong, X., Liu, H., and Zhou, Y. (2013). "Numerical simulation of the seismic response of the Zipingpu concrete face rockfill dam during the Wenchuan earthquake based on a generalized plasticity model." Comput. Geotech., 49(0), 111–122.